Polymer 51 (2010) 355–367

Contents lists available at ScienceDirect

Polymer

journal homepage: www.elsevier.com/locate/polymer

# RAFT polymerization and self-assembly of thermoresponsive poly(*N*-decylacrylamide-*b*-*N*,*N*-diethylacrylamide) block copolymers bearing a phenanthrene fluorescent α-end group

Telmo J.V. Prazeres [a,b], Mariana Beija [a,b,1], Marie-Thérèse Charreyre [a,*], José Paulo S. Farinha [b], José M.G. Martinho [b,**]

[a] Unité Mixte CNRS-bioMérieux, École Normale Supérieure de Lyon, 46 Allée d'Italie, 69364 Lyon Cedex 07, France
[b] Centro de Química-Física Molecular and IN – Institute of Nanoscience and Nanotechnology, Instituto Superior Técnico, Av. Rovisco Pais 1, 1049-001 Lisboa, Portugal

ARTICLE INFO

*Article history:*
Received 30 September 2009
Received in revised form
20 November 2009
Accepted 25 November 2009
Available online 3 December 2009

*Keywords:*
RAFT polymerization
Thermoresponsive block copolymers
Fluorescence

ABSTRACT

Phenanthrene α-end-labeled poly(*N*-decylacrylamide-*b*-*N*,*N*-diethylacrylamide) ($PDcA_n$-*b*-$PDEA_m$) block copolymers consisting in a highly hydrophobic block ($n = 11$) and a thermoresponsive block with variable length ($79 \leq m \leq 468$) were synthesized by reversible addition-fragmentation chain transfer (RAFT) polymerization. A new phenanthrene-labeled chain transfer agent (CTA) was synthesized and used to control the RAFT polymerization of a hydrophobic acrylamide derivative, *N*-decylacrylamide (DcA). This first block was further used as macroCTA to polymerize *N*,*N*-diethylacrylamide (DEA) in order to prepare diblock copolymers with the same hydrophobic block of PDcA (number average molecular weight: $M_n = 2720\ g\ mol^{-1}$, polydispersity index: $M_w/M_n = 1.13$) and various PDEA blocks of several lengths ($M_n = 10{,}000$–$60{,}000\ g\ mol^{-1}$) with a very high blocking efficiency. The resulting copolymers self-assemble in water forming thermoresponsive micelles. The critical micelle concentration (CMC) was determined using Förster resonance energy transfer (FRET) between phenanthrene linked at the end of the PDcA block and anthracene added to the solution at a low concentration ($10^{-5}$ M), based on the fact that energy transfer only occurs when phenanthrene and anthracene are located in the core of the micelle. The CMC (~2 μM) was obtained at the polymer concentration where the anthracene fluorescence intensity starts to increase. The size of the polymer micelles decreases with temperature increase around the lower critical solution temperature of PDEA in water (LCST ~ 32 °C) owing to the thermoresponsiveness of the PDEA shell.



## 1. Introduction

Labeling of polymers with fluorescent groups is an appropriate and useful tool to study intra and intermolecular polymer chain interactions [1–3], to follow coil-to-globule transition [4–6], self-assembly of block copolymers in selective solvents [7], as well as to characterize the interfaces in polymer blends [8] and the morphology of thin polymer films [9]. They can also be used as probes in fluorescence microscopy and imaging [10] and as light-harvesters in solar cells [11].

Polymers bearing fluorophores distributed randomly along the polymer chain can be obtained either by polymerizing statistically a small quantity of a fluorescent comonomer [12] or by labeling polymer precursors with fluorescent dye derivatives [12,13]. However, these synthetic methodologies do not produce polymers with fluorophores located at a specific position such as one or both chain-ends [3,14], or at the common junction of diblock copolymers [7,15,16].

The first monodisperse well-defined polymers bearing a fluorophore at a specific position of the chain were prepared by living anionic polymerization using several strategies: use of a fluorescent labeled initiator [16]; reaction of the functional polymer chain-end with a dye derivative [17]; insertion of a fluorophore at the chain-end by a termination labeling reaction [18] and using a bifunctional fluorescent terminator to label diblock copolymers at the junction point [19].

* Corresponding author. Present address: Laboratoire Joliot-Curie et Laboratoire Ingénierie des Matériaux Polymères, ENS, IFR128, 46 Allée d'Italie 69364 Lyon Cedex 07, France. Tel.: +33 4 72 72 89 38; fax: +33 4 72 72 87 87.
** Corresponding author. Tel.: +351 218419250; fax: +351 218464455.
*E-mail addresses:* mtcharre@ens-lyon.fr (M.-T. Charreyre), jgmartinho@ist.utl.pt (J.M.G. Martinho).
[1] Present address: Laboratoire des Intéractions Moléculaires et Réactivité Chimique et Photochimique, UMR 5623, Université Paul Sabatier, 31062 Toulouse Cedex 9, France.

0032-3861/$ – see front matter © 2009 Elsevier Ltd. All rights reserved.
doi:10.1016/j.polymer.2009.11.055

The developments of controlled/living free radical polymerization (CRP) [20] in the last decade have opened up the opportunity to prepare monodisperse polymers from a much larger variety of monomers than anionic polymerization, under milder and simpler polymerization conditions [21]. Well-defined polymers bearing a fluorophore at a specific site were obtained either by post-modification of the polymer chain or by using a previously labeled initiator/chain transfer agent.

The post-modification strategy was successfully used to obtain polymers end-capped with a fluorophore, synthesized by both the reversible addition-fragmentation chain transfer (RAFT) polymerization [22–25], and nitroxide-mediated free radical polymerization (NMP) [26,27], while atom transfer radical polymerization (ATRP) was used to prepare $C_{60}$ end-labeled poly(styrene) and poly (methylmethacrylate) [28,29]. "Click" chemistry was also applied to synthesize a coumarin end-labeled poly(vinylacetate) by RAFT polymerization [30]. However, to reach adequate labeling yields (80–100%) by the post-modification approach, a good accessibility of the polymer reactive end-group is needed (solely obtained for short polymer chains in good solvents), so that a very large excess of fluorophore is often required.

In order to circumvent the low yield of labeling, several strategies have been proposed based on fluorescent labeled initiators or chain transfer agents. Perylene, pyrene and dansyl modified alcoxyamines for NMP were synthesized and used for styrene and *n*-butylacrylate polymerization [31–34], while pyrene [14,35] and fluorescein [36] labeled initiators were successfully used in ATRP polymerization. Polymers labeled at the junction between the two blocks were also synthesized by both ATRP [37] and NMP [38], using bifunctional initiators. End-functionalized fluorescent polymers have already been synthesized by RAFT polymerization using fluorescent labeled RAFT agents. For instance, they were prepared through carboxylic acid activation of a RAFT agent followed by reaction with an alcohol-derived fluorophore [39], by reacting the RAFT agent with a fluorophore-labeled monomer in a 1:1 molar ratio [40,41], by the reaction of $CS_2$ and a chloromethyl-derived fluorophore in basic media in the presence of a phase transfer agent [42] and by a two step procedure involving an amino-derived fluorophore and 2-bromopropionic bromide followed by reaction with a dithiobenzoate salt [43].

In this work, a phenanthrene-functionalized RAFT agent was synthesized from a precursor dithioester [44] and further used to prepare a series of amphiphilic block copolymers of poly(*N*-decylacrylamide-*b*-*N*,*N*-diethylacrylamide), PDcA-*b*-PDEA, phenanthrene-labeled at the α-chain-end. RAFT was chosen among the CRP methodologies, since it is a well established technique for the polymerization of acrylamide derivatives leading to well-controlled architectures and high molecular weights [45–50]. The block copolymers were prepared by a sequential method, where the first block (bearing a dithiobenzoate group at the ω-chain-end), was used as macro chain transfer agent (macroCTA) to control the polymerization of the second monomer [47,48] which mediated preparation of well-defined block copolymers with the same hydrophobic block length and several hydrophilic blocks of varying molecular weight. The DcA monomer unit of the hydrophobic block has an alkyl chain short enough to obtain micellar aggregates with a relatively fluid hydrophobic core [51]. On the other hand, the hydrophilic block of PDEA is thermoresponsive in water, with a lower critical solution temperature (LCST) around 30–33 °C for its heteroactic form [52–56]. Since PDEA is a biocompatible polymer [57,58], it may be more suitable than the well known poly(*N*-isopropylacrylamide) (PNIPAM) for some biological applications [59,60], due to the absence of the active hydrogen in the amide group [57].

The ability of the PDcA-*b*-PDEA block copolymers to self-assemble in water at several temperatures below and above LCST of the PDEA block was investigated. The critical micelle concentration (CMC) was determined using the Förster resonance energy transfer (FRET) between phenanthrene linked at the α-end of the PDcA block and anthracene added to the solution at a low concentration ($10^{-5}$ M). Above the CMC, the anthracene migrates to the core of the micelles and energy transfer occurs with a consequent increase of anthracene fluorescence intensity. In addition, the variation of size of the polymer micelles with temperature above the volume phase transition temperature ($T_{VPT} \sim 32$ °C) of the thermosensitive PDEA shell was investigated by dynamic light scattering (DLS).

## 2. Experimental section

### 2.1. Materials

*N*-acryloyl chloride (Aldrich, 96%) was distilled (90 °C) prior to use. *N*,*N*-diethylacrylamide (DEA) (Monomer–Polymer & Dajac Labs.) was distilled under reduced pressure (110 °C). 2,2′-azobis (isobutyronitrile) (AIBN, Fluka, 98%) and 2,2′-azobis(2,4-dimethylvaleronitrile) (V-65, WAKO, 98%) were purified by recrystallization from ethanol. 1,4-Dioxane (Acros, 99%) was distilled over $LiAlH_4$ (110 °C), THF (Aldrich, 99%) was distilled over $CaH_2$. Triethylamine (Aldrich, 99.5%), decylamine (Aldrich, 95%) and trioxane (Acros, 99%) were used as received. All other chemicals were obtained from several sources and used as received.

### 2.2. Synthesis of N-decylacrylamide (DcA)

This hydrophobic monomer was synthesized according to the procedure reported by D'Agosto et al. for an acrylate derivative [61]. *N*-decylamine (47.9 g, 28.9 mmol) and triethylamine (32.4 g, 31.8 mmol) were dissolved in 300 mL of $CH_2Cl_2$. Acryloyl chloride was then added dropwise (29.0 g, 32.0 mmol) over a period of 1 h 30 min, keeping temperature below 2 °C. The mixture was washed with saturated $NH_4Cl$ aqueous solution, $NaHCO_3$ aqueous solution and brine, dried over anhydrous $MgSO_4$ and filtered. A yellowish powder was obtained after solvent evaporation. The product was isolated as white crystals after several recrystallizations from pentane. Yield: 70%. $^1$H NMR (200 MHz, $CDCl_3$) ppm, $\delta$ 0.88 (3H, t, $-CH_2CH_2$ $(CH_2)_7CH_3$); 1.26 (14H, *broad*, $-CH_2CH_2$ $(CH_2)_7CH_3$); 1.43 (2H, m, $-CH_2CH_2(CH_2)_7CH_3$); 3.31 (2H, dt, $-CH_2CH_2(CH_2)_7CH_3$); 5.58–5.64 (1H, dd, –C(*H*)H═CH); 5.92 (1H, *broad*, –N*H*); 6.04–6.18 (1H, dd, –C(H)H═C*H*); 6.18–6.33 (1H, dd, –C(H)*H*═CH).

### 2.3. Synthesis of N-[4-(9-phenanthrenyl)butyl-2-(2-phenyl-1-thioxo)thio]-propanamide (PBTP)

The succinimido-2-[[2-phenyl-1-thioxo]thio]-propanoate (precursor RAFT agent **1**) [44] and 4-(9-phenanthrenyl)butyl amine hydrochloride (**2**) [62] were synthesized according to reported literature procedures. In a round-bottom flask, the precursor RAFT agent **1** (0.72 g, 1.72 mmol) and 4-(9-phenanthrenyl)butyl amine hydrochloride **2** (0.47 g, 1.64 mmol) were dissolved in chloroform (140 mL). A solution of triethylamine (0.19 g, 1.89 mmol) in 28.5 mL of chloroform was then added dropwise. The reaction mixture was stirred at 30 °C until the end of the addition (*ca.* 1 h 30 min), then it was left to react for another 30 min. The final mixture was concentrated to around 100 mL, washed five times with 200 mL of distilled water (to remove *N*-hydroxysuccinimide, NHS), dried over anhydrous $MgSO_4$ and filtered. After solvent removal, the product was purified by silica gel chromatography using chloroform/cyclohexane mixture (8:2 v/v) as eluent to recover an orange solid. Yield: 65%. ($C_{28}H_{27}NOS_2$; $M_r = 457.65$ g mol$^{-1}$). Calcd: C 73.48, H 5.95, N 3.06, S 14.01. Found: C 72.98, H 5.88, N 2.92, S 13.75. MS (FAB) found ($M - H^+$): 458.1650 *m*/*z*; calcd: 458.1612 *m*/*z*. $^1$H NMR (200 MHz,

$CDCl_3$) ppm, $\delta$ 1.60–1.90 (4H, m + m, –Phe–$CH_2(CH_2)_2CH_2NH$); 1.65–1.82 (3H, d, –C(=O)CH($CH_3$)S); 3.10 (2H, t, Phe–$CH_2(CH_2)_2CH_2NH$); 3.32 (2H, m, Phe–$CH_2(CH_2)_2CH_2NH$); 4.67 (1H, q, –C(=O)CH($CH_3$)S); 6.39 (1H, *broad*, Phe–$CH_2(CH_2)_2CH_2NH$); 7.32 (2H, dd, –$CS_2$-aryl (meta)); 7.40–7.70 (1H, –$CS_2$-aryl (para); 5H, Phe); 7.76 (1H, m, Phe); 7.90 (2H, d, –$CS_2$-aryl (ortho)); 8.04 (1H, m, Phe); 8.65–8.71 (2H, m, Phe). $^{13}$C NMR (50 MHz, $CDCl_3$) ppm, $\delta$ 16.13 (–C(=O)CH($CH_3$)S); 27.20 (Phe–$CH_2CH_2CH_2CH_2NH$); 29.31 (Phe–$CH_2CH_2CH_2CH_2NH$); 32.85 (Phe–$CH_2CH_2CH_2CH_2NH$); 39.48 (Phe–$CH_2CH_2CH_2CH_2NH$); 48.46 (–C(=O)CH($CH_3$)S); 122.37, 123.17, 124.29, 125.92 (Phe, 4 CH); 126.05 (Phe, 1 CH); 126.11 (Phe, 1 CH); 126.53 (Phe, 2 CH); 126.96 (–$CS_2$-aryl (ortho)); 128.04 (Phe, 1 CH); 128.38 (–$CS_2$-aryl (meta)); 129.08, 129.55, 130.63, 131.78 (Phe, 4 CH); 132.92 (–$CS_2$-aryl (para)); 136.10 (Phe $C_5$); 144.21 (–$CS_2$-aryl C); 170.33 (–C(=O)CH($CH_3$)S); 227.63 (–$CS_2$-aryl). UV–vis (in THF): band at $\lambda_{max} = 299$ nm ($\varepsilon = 22{,}400$ mol$^{-1}$ L cm$^{-1}$).

### 2.4. Synthesis of α-phenanthrene-end-labeled poly (N-decylacrylamide) (Phe-PDcA macroCTA)

DcA (5.0 g, 23.8 mmol), PBTP (0.29 g, 0.64 mmol), AIBN (10 mg, 0.063 mmol), 1,4-dioxane (23.7 mL), and trioxane (0.19 g, internal reference for $^1$H NMR determination of monomer conversion) were introduced in a Schlenk tube equipped with a magnetic stirrer [49] The mixture was deoxygenated by four freeze-pump-thaw cycles and then heated under nitrogen in a thermostated oil bath at 90 °C. For kinetics study, samples were periodically withdrawn from the polymerization medium and the monomer conversion was determined by $^1$H NMR, using as internal reference the trioxane protons [63]. The polymerization was stopped after 1 h 30 min by cooling under liquid nitrogen. The obtained polymer was precipitated into a mixture of MeOH/$H_2O$ (3:1 v/v) to remove the unreacted monomers, filtered and dried under vacuum. The complete elimination of residual monomers was confirmed by $^1$H NMR.

### 2.5. Synthesis of α-phenanthrene-end-labeled poly(N-decylacrylamide-b-N,N-diethylacrylamide) (Phe-PDcA-b-PDEA)

Typically, the RAFT polymerization of DEA was carried out in a Schlenk tube equipped with a magnetic stirrer by dissolving DEA, Phe-PDcA, V-65 and trioxane in 1,4-dioxane. The mixture was deoxygenated by four freeze-pump-thaw cycles. Under nitrogen, it was heated in a thermostated oil bath at 70 °C. For all experiments, the initial monomer concentration was kept equal to 3.8 mol L$^{-1}$. All copolymers (BC1 to BC5) were precipitated in petroleum ether (3 times) in order to remove unreacted monomer and possible Phe-PDcA dead chains. The final copolymers were recovered by filtration and dried under vacuum. The complete elimination of residual monomers was confirmed by $^1$H NMR.

### 2.6. Elimination of the thiocarbonylthio ω-end group from Phe-PDcA-b-PDEA block copolymers by aminolysis

The thiocarbonylthio moiety at the ω-end of Phe-PDcA-*b*-PDEA block copolymers was converted into a thiol by treating the copolymers with a large excess of hexylamine (~100 eq relatively to the chain-end) in dichloromethane at room temperature during ~4 h (aminolysis reaction) [64]. The treated copolymers were precipitated several times in hexane in order to remove the excess of hexylamine and the secondary product from the aminolysis reaction. The orange or rose copolymers became white once having the thiol function at the ω-terminus. The absorption spectra of the treated copolymers were characteristic of phenanthrene, not showing the absorption of the thiocarbonylthio moiety. The conversion of the thiocarbonylthio group to a thiol was further confirmed by the phenanthrene derivative lifetime in THF that is close to the value of the unquenched phenanthrene (~47 ns) [65].

### 2.7. Preparation of samples for DLS and determination of CMC by fluorescence

The aqueous solutions of copolymers used to determine the critical micelle concentration (CMC) by fluorescence and for the DLS experiments (after removing the thiocarbonylthio group) were prepared by using the solvent-assisted solubilization method in order to obtain monodisperse micelles, to prevent the presence of some large aggregates. THF was used because it is a good solvent for both blocks.

Concentrated solutions (~75 g L$^{-1}$) of copolymers BC1–BC5 were prepared in THF. Then, to a small volume of these concentrated solutions (previously transferred into small vials (or light scattering tubes) immersed in an ice bath, ~2 °C), cold water was added dropwise with gentle agitation to the required final volume. The final solutions contained always less than 2% v/v of THF. Some control experiments were performed and they indicated that the low THF content does not interfere significantly with the properties of the micellar aggregates [66]. The final aqueous solutions were always let to equilibrate (and stored) at 4 °C, for at least 24 h.

### 2.8. Instrumentation

Both $^1$H NMR (200 MHz) and $^{13}$C NMR (50 MHz) spectra were recorded on a Bruker AC 200 spectrometer at 300 K in chloroform-*d* ($CDCl_3$).

The mass spectra (SCA, CNRS, Solaize, France) were obtained on a ZAB2-SEQ spectrometer (VG, Manchester, UK) using fast atom bombardment ionization.

The absorption spectra were recorded on a Shimadzu UV-3101PC UV–vis–NIR spectrophotometer using square quartz cells of 1 cm path length.

The MALDI-ToF MS analyses (SCA, CNRS, Solaize, France) were recorded on a Voyager-DE STR (Applied Biosystems) spectrometer equipped with a nitrogen laser (wavelength 337 nm). The accelerating voltage was 20 kV and the positive ions were detected. The spectra were the sum of 200 shots, and an external mass calibration was used (mixture of peptides standards, Sequazyme kit). The samples were deposited on a stainless steel target and dried. Samples were prepared by dissolving 10 g L$^{-1}$ of polymer in freshly distilled tetrahydrofuran (THF). The matrix was 3-β-indole acrylic acid (IAA, Fluka, Milwaukee, WI), used without further purification and dissolved in distilled THF (10 g L$^{-1}$). Matrix and polymer solutions were mixed at a volume ratio of 9:1; then 1 μL of the mixture was deposited onto the MALDI target before insertion into the ion source chamber.

The molecular weight distributions of the hydrophobic polymer (Phe-PDcA macroCTA) and the block copolymers were obtained by size exclusion chromatography (SEC) with THF eluent, using a Waters 1515 isocratic HPLC pump with a flow rate of 1 mL min$^{-1}$, a Waters 2410 refractive index detector and a Styragel HR4E column. The relative molecular weights of the Phe-PDcA macroCTA were obtained using polystyrene standards.

The absolute molecular weights of the Phe-PDcA-*b*-PDEA block copolymers were obtained by SEC in DMF using both a differential refractive index and a multi-angle light scattering (miniDAWN TREOS from Wyatt) detectors. The differential refractive index of the block copolymer was set equal to the value of PDEA in DMF, d*n*/d*C* = 0.081 mL g$^{-1}$.

Fluorescence spectra were acquired with a SLM-AMINCO 8100 Series 2 spectrofluorometer using a bandwidth of 4 nm for the emission and excitation, in 5 × 5 mm quartz cuvettes.

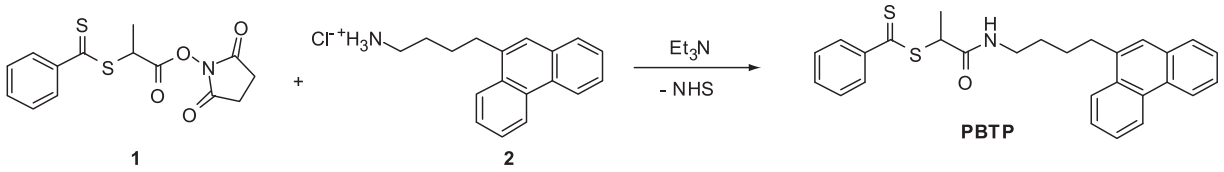


**Scheme 1.** Synthesis of the fluorescent RAFT agent *N*-[4-(9-Phenanthrenyl)butyl-2-(2-phenyl-1-thioxo)thio]-propanamide (PBTP).

The hydrodynamic diameter of the micellar aggregates was obtained by dynamic light scattering using a Brookhaven Instruments (BI-200SM Goniometer and BI-9000 AT autocorrelator) with a He–Ne laser (632.8 nm, 35 mW) from Spectra Physics and an avalanche photodiode as detector. The measurements were performed with $\sim 1.4\ g\ L^{-1}$ of polymer solutions in MQ-Water. The autocorrelation functions were analyzed both by Laplace inversion (CONTIN) and Expsam V3.0 programs included in the BI-ZP software package from Brookhaven.

## 3. Results and discussion

### 3.1. Synthesis of a Phe-labeled RAFT agent

A novel phenanthrene-labeled RAFT agent was synthesized by a one step amidation following a previously reported procedure [44] involving a precursor RAFT agent (bearing an activated ester function) and an amino derivative (Scheme 1). The originality of this strategy is based on the highly favorable reactivity of the activated carbonyl group in comparison with the thiocarbonyl group towards primary amines, so that the thioamidation side-reaction can be completely avoided. Moreover, the resulting dye-labeled RAFT agent bears a stable peptidic bond between the dye moiety and the dithioester function.

As the ammonium chloride form of the phenanthrene derivative was not reactive in the presence of the precursor dithioester **1**, triethylamine was added to induce *in situ* deprotonation that led to the quantitative formation of dye-labeled dithiobenzoate, *N*-[4-(9-Phenanthrenyl)butyl-2-(2-phenyl-1-thioxo)thio]-propanamide (PBTP). After purification by silica gel chromatography, a final yield of 65% was obtained, similar to those reported for other functional RAFT agents synthesized from the same precursor [44]. In the literature, other dye-labeled RAFT agents were synthesized with yields in the range of 21–92% for dyes introduced in the *R* group [40–43,67] of the thiocarbonylthio compound and 20–63% for dyes introduced in the *Z* group [68].

The structure of PBTP was confirmed by FAB mass spectrometry, $^1H$ and $^{13}C$ NMR whereas micro-analysis indicated a very good purity (see experimental part). This dye-labeled dithioester is the first RAFT agent bearing a phenanthrene moiety in the *R* group *i.e.* leading to α-phenanthrene-labeled polymer chains.

### 3.2. Synthesis and characterization of Phe-PDcA homopolymers

The fluorescent RAFT agent PBTP was used to control the polymerization of *N*-decylacrylamide, DcA (Scheme 2). The polymerization was carried out in 1,4-dioxane at 90 °C, using 2,2′-azobis(isobutyronitrile) (AIBN) as initiator. In order to minimize the number of chains initiated by AIBN, the ratio [PBTP]/[AIBN] was kept equal to 10. The initial concentration of monomer was $[DcA]_0 = 1\ mol\ L^{-1}$ to get a complete solubilization of the monomer in 1,4-dioxane (at 30 °C).

The kinetics of the RAFT polymerization of DcA mediated by PBTP was followed by $^1H$ NMR [63]. The monomer conversion was obtained from Eq. (1), where $A_t$ is the integral of the peak corresponding to one vinylic proton of DcA (at 5.6 ppm) and $A_0$ is the integral of the peak corresponding to the six trioxane protons (at 5.1 ppm).

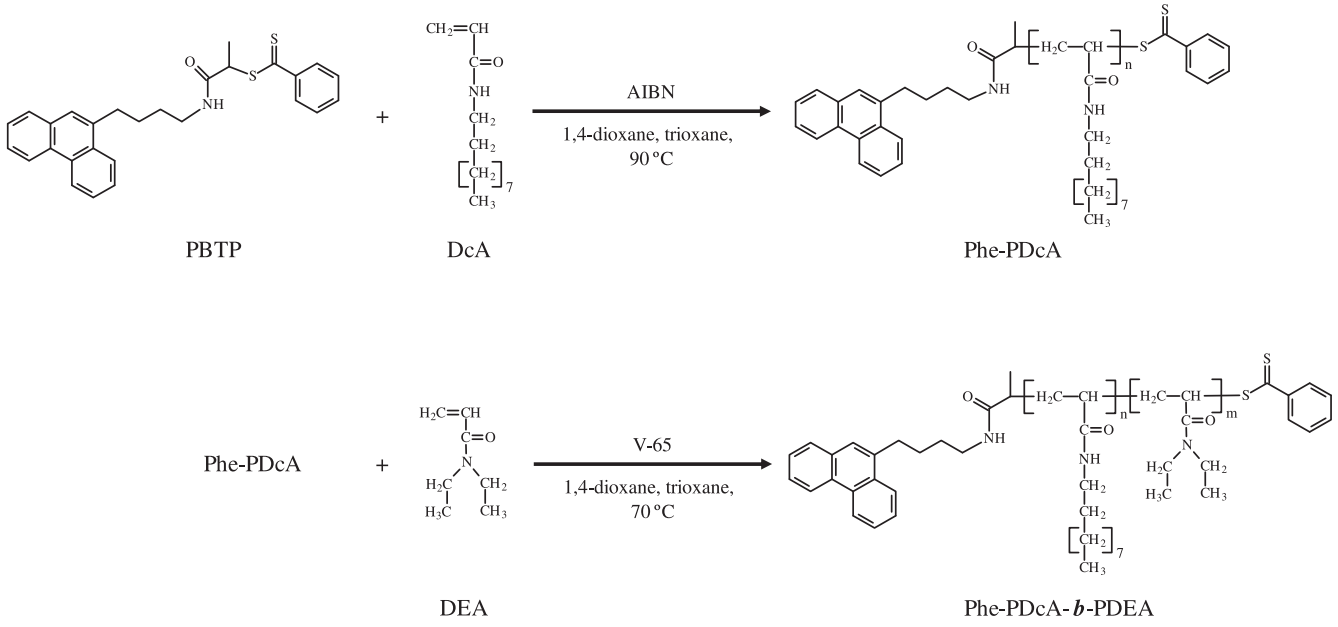


**Scheme 2.** Synthesis of the amphiphilic block copolymers Phe-PDcA-*b*-PDEA.

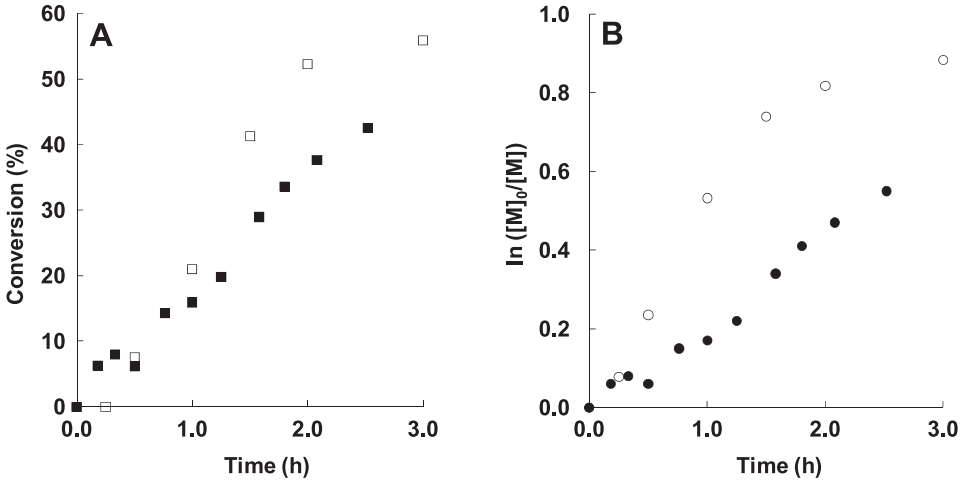


**Fig. 1.** Monomer conversion *vs* time (A) and pseudo-first order kinetics (B) for the RAFT polymerization of DcA mediated by *t*BDB (open symbols) and PBTB (closed symbols).

$$\text{Conversion}(\%) = \left[1 - \frac{A_t}{A_0/6}\right] \times 100 \quad (1)$$

A conversion of about 45% was reached in approximately 3 h (Fig. 1A) with a linear variation of the ln([$M_0$]/[$M$]) with time during the first 2 h of polymerization (Fig. 1B). In comparison with a run in the presence of *tert*-butyl dithiobenzoate, *t*BDB, in similar conditions [69], kinetics were slower with phenanthrene-labeled dithiobenzoate, which might be attributed to a lower re-initiation efficiency of the fragment radical hindered by the bulky phenanthrene group. However, such phenomenon had not been observed for similar functional RAFT agents bearing a biotin or a protected carbohydrate or a phospholipid moiety, instead of a phenanthrene derivative [44].

The SEC chromatograms at different conversions are shown in Fig. 2A. The peaks are rather symmetrical with a slight tail (indicating some termination reactions and/or some degradative transfer reactions) and some residual monomer at conversions below 20%. The $M_n$ values (relative to PS standards) vary linearly with monomer conversion, with polydispersity index, $M_w/M_n \leq 1.2$ (Fig. 2B). The linear variation of the relative $M_n$ values with conversion and the low polydispersity indexes indicate that DcA polymerization is efficiently controlled by the new fluorescent RAFT agent, PBTP.

The sample of phenanthrene end-labeled poly(*N*-decylacrylamide) that was further used to synthesize block copolymers was obtained at 21% conversion which, according to Eq. (2) [45],

$$M_n^{calc} = \frac{[M]_0 \cdot MW_m \cdot \text{Conversion}}{[\text{CTA}]_0} + MW_{CTA} \quad (2)$$

gave a theoretical $M_n$ value of 2100 g mol$^{-1}$, corresponding to an average polymerization degree of $X_n = 8$ (with $MW_m$ and $MW_{CTA}$ the molecular weights of monomer and CTA, respectively).

The $^1$H NMR spectrum of this Phe-PDcA sample (after purification) is shown in Fig. 3 with the proton assignments corresponding to the monomer unit, the phenanthrene α-end group and the dithiobenzoate ω-end group, attributed by comparison with the $^1$H NMR spectrum of the phenanthrene-labeled RAFT agent. The average polymerization degree $X_n$ was then calculated by comparison of the integral of the characteristic peak corresponding to two phenanthrene aromatic protons ($2H_{Phe}$) at 8.60–8.80 ppm, with the integral of the band at 2.9–3.6 ppm, which corresponds to $2X_nH_e + 2H_5 + 2H_2$. Even though that integral contained the contribution from protons of the phenanthrene linker ($H_2$ and $H_5$), it was as the best choice for determining $X_n$, since the integrals corresponding to the protons *g* and *h* were not well-defined due to overlap of the peaks from other protons. From the value obtained for the integral, we calculated $X_n = 9.4$, corresponding to a number average molecular weight of 2445 g mol$^{-1}$.

MALDI-TOF MS analysis of this Phe-PDcA sample was also performed to obtain the number average molecular weight and to determine the chain-end functionalities (Fig. 4). From the mass spectrum obtained in the linear mode (not shown), one was able to

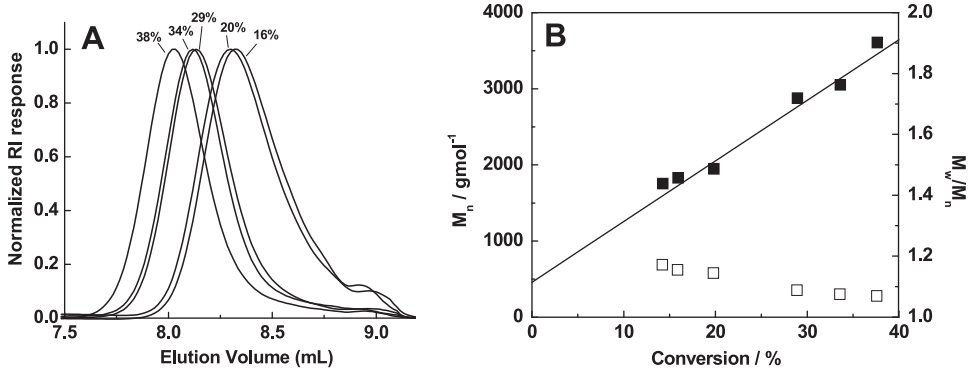


**Fig. 2.** (A) Evolution of the normalized SEC traces in THF for the RAFT polymerization of DcA mediated by the chain transfer agent PBTP at different conversions. (B) Plots of $M_n$ (filled squares) and $M_w/M_n$ (empty squares) values *vs* monomer conversion for DcA polymerization in 1,4-dioxane at 90 °C in the presence of PBTP: $[DEA]_0 = 1$ mol L$^{-1}$;$[PBTP]_0/[AIBN]_0 = 10$. The line represents the expected values calculated using Eq. (2).

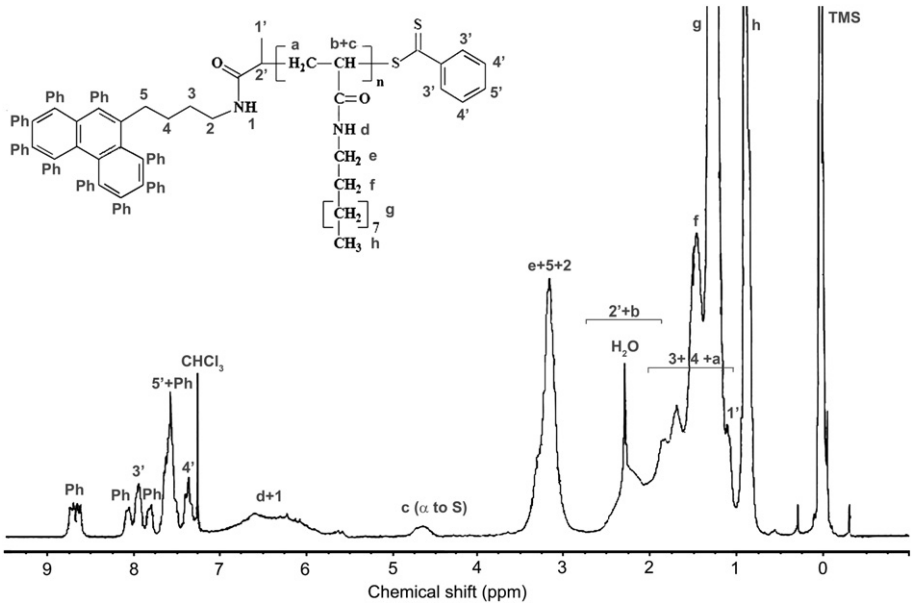


**Fig. 3.** $^{1}$H NMR spectrum of PDcA homopolymer (200 MHz, $CDCl_3$, 300 K); proton assignment (ppm): 0.7–1.0 ($3nH_h$); 1.1–1.2 ($3H_{1'}$); 1.26 ($14nH_g$); 1.0–2.0 ($2nH_a$); 1.46 ($2nH_f$); 1.6–1.9 ($2H_3 + 2H_4$); 1.8–2.6 ($(n-1)H_b$); 1.9–2.6 ($3H_{2'}$); 2.9–3.6 ($2nH_e + 2H_5 + 2H_2$); 4.5–4.7 ($1H_c$); 5.5–7.1 (*broad*, $nH_d + 1H_1$); 7.39 ($2H_{4'}$); 7.62 ($1H_{5'} + 5H_{Ph}$); 7.82 ($1H_{Ph}$); 7.95 ($2H_{3'}$); 8.07 ($1H_{Ph}$); 8.60–8.80 ($2H_{Ph}$).

determine the number average molecular weight ($M_n$ = 2720 g mol$^{-1}$) and the polydispersity index (1.13). The difference between two main peaks (Δ) of the distribution (211.2 *m*/*z*) corresponds to the DcA ($C_{13}H_{25}NO$) repeating unit (211.34 g mol$^{-1}$).

The mass spectrum obtained in the reflectron mode (Fig. 4A) has a sufficient resolution to resolve single isotope peaks. By selecting $X = 8$, one can clearly see the isotopic patterns for individual polymer chains (Fig. 4B). It is possible to distinguish at least 12 isotopic patterns and for most of them a molecular structure could be assigned (Table 1). The accuracy given by the spectrometer used in this study is 0.008% (in the reflectron mode) that corresponds to ±0.2 mass units for a polymer chain of 2170 mass units.

The expected isotopic distribution for each population must have a similar shape to that calculated for the ion $[C_{21}H_{22}NO–(C_{13}H_{25}NO)_8–C_7H_5S_2 + Na]^+$, where $X = 8$, shown in the inset of Fig. 4B. There is a good agreement between the simulated isotopic pattern and the one obtained experimentally. The main population, P4, corresponds to a chain with the expected structure $[C_{21}H_{22}NO–(C_{13}H_{25}NO)_8–C_7H_5S_2 + Na]^+$ which confirms the presence of the phenanthrene fluorophore at the α-end and the dithiobenzoate

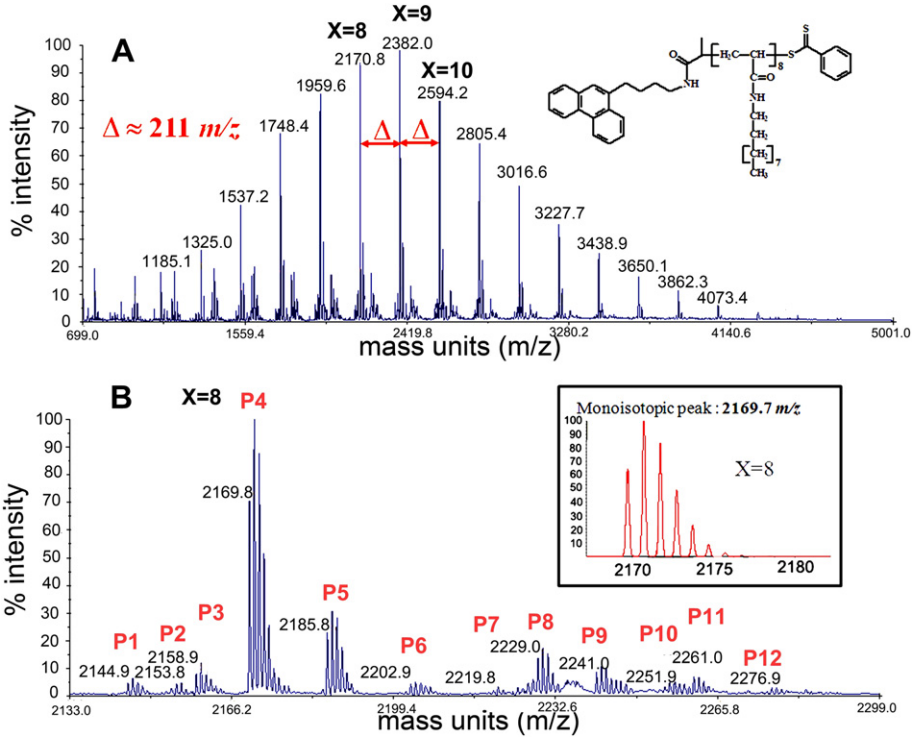


**Fig. 4.** (A) MALDI-TOF mass spectrum of Phe-PDcA in the reflectron mode. (B) Enlarged region of MALDI-TOF mass spectrum shown in A for the polymerization degree $X = 8$ and attribution of populations (Table 1). Inset: calculated isotopic pattern ($C_{132}H_{227}N_9O_9S_2Na$).

**Table 1**
Structures corresponding to the assigned peaks in Fig. 4.

| Peak | Monoisotopic mass | | Structure | Cationization | *X* |
|---|---|---|---|---|---|
| | Experimental | Theoretical | | | |
| P1 | 2144.9 | 2144.8 | 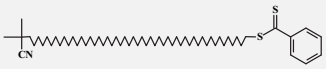 | Na | 9 |
| P2 | 2153.8 | 2153.7 | 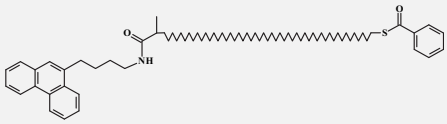 | Na | 8 |
| P3 | 2158.9 | 2160.8 | 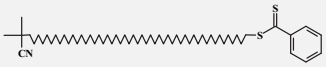 | K | 9 |
| | | 2169.7 | 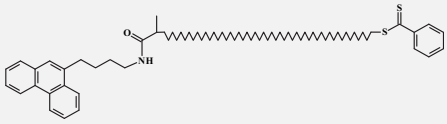 | Na | 8 |
| P4 | 2169.8 | | | | |
| | | 2169.7 | 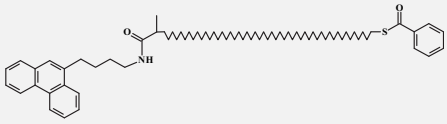 | K | 8 |
| P5 | 2185.8 | 2185.7 | 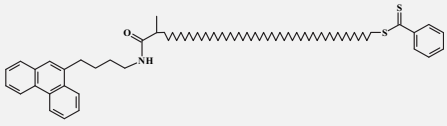 | K | 8 |
| | | 2202.0 |  | Na | 10 |
| P6 | 2202.9 | | | | |
| | | 2204.0 | 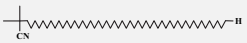 | Na | 10 |
| P7 | 2219.8 | 2220.0 | 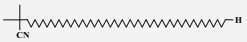 | K | 10 |
| | | 2226.9 | 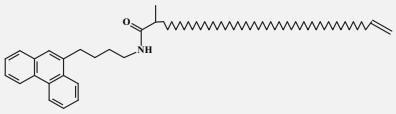 | Na | 9 |
| P8 | 2229.0 | | | | |
| | | 2229.0 | 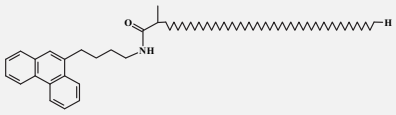 | Na | 9 |
| | | 2242.9 | 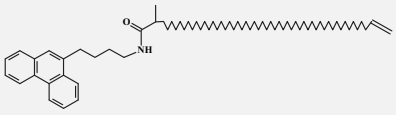 | K | 9 |
| P9 | 2241.0 | | | | |
| | | 2244.9 | 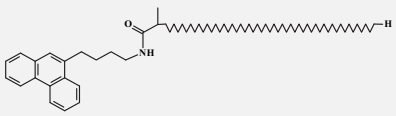 | K | 9 |

(*continued on next page*)

**Table 1** (*continued*)

| Peak | Monoisotopic mass | | Structure | Cationization | *X* |
|---|---|---|---|---|---|
| | Experimental | Theoretical | | | |
| P10 | *2251.9* | NA | NA | NA | NA |
| P11 | 2261.0 | 2260.9 | 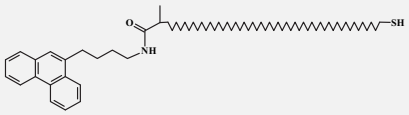 | Na | 9 |
| P12 | 2276.9 | 2276.9 | 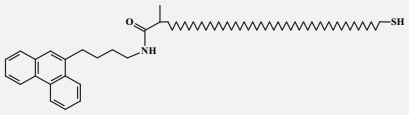 | K | 9 |

X: polymerization degree of the considered chain; NA: non attributed.

moiety (*Z* group of the macroCTA) at the $\omega$-end (dormant chains). The monoisotopic peak is at 2169.8 mass units for a calculated value of 2169.7 mass units. It is worth mentioning here that the C–S bond of the dormant end-group is not as sensitive in a polyacrylamide derivative synthesized by RAFT process than in a polystyrene, that makes possible analyses by MALDI-TOF MS as we have already demonstrated for several kinds of polyacrylamide derivatives [64,70] The second main population, P5, corresponds to the same chains but cationized with $K^+$. The populations P1 and P3 may be attributed to chains initiated by AIBN with $X = 9$ ($Na^+$ and $K^+$ cationization) [71]. A very small amount of dormant chains where the dithioester group was oxidized to a thioester group are present as population P2 (and probably some contribution in population P4), which was observed previously for poly(*N*-acryloylmorpholine) (PNAM) [64], poly(*N*-*tert*-butylacrylamide) (PTBAm) [70], and poly(methylmethacrylate) (PMMA) [72]. Population P8 can be attributed to dead chains initiated by PBTP and terminated by a proton ($Na^+$ cationization). They can result either from termination reactions by disproportionation, transfer reactions or fragmentation in the spectrometer [64]. In the case of the chains resulting from disproportionation, the corresponding chains ended by a double bond are expected at 2226.9 and 2242.9 mass units, however this structure could not be attributed to any peak. The corresponding chains cationized by $K^+$ could not be accurately assigned (P9). Populations P6 and P7 can be attributed to dead chains initiated by AIBN and terminated by a proton ($Na^+$ and $K^+$ cationization, respectively). Population P10 could not be attributed, whereas populations P11 and P12 could be attributed to thiol terminated chains ($Na^+$ and $K^+$ cationization, respectively) possibly resulting from hydrolysis or aminolysis of some dormant chains [64].

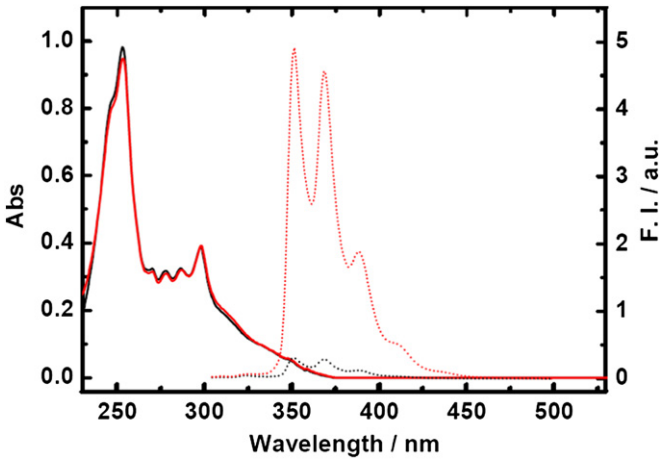


**Fig. 5.** Absorption (solid lines) and fluorescence (dashed lines) of PBTP RAFT agent (black lines) and Phe-PDcA homopolymer (red lines). The solutions present the same absorbance at 299 nm. (For interpretation of the references to colour in this figure legend, the reader is referred to the web version of this article.)

The MALDI-TOF mass spectrum confirms the presence of the phenanthrene fluorophore at the $\alpha$-end and the dithiobenzoate moiety at the $\omega$-end of the PDcA chain. Since MALDI-TOF mass analysis gives a more accurate $M_n$ value (2720 g mol$^{-1}$) than NMR, it was used to determine the molar extinction coefficient of the macroCTA at 299 nm, $\varepsilon^{299}_{\text{macroCTA}} = 29,740$ mol$^{-1}$L cm$^{-1}$.

Fig. 5 shows the absorption and emission spectra of PBTP and Phe-PDcA in THF. In both absorption spectra, the characteristic absorption of the phenanthrene (below 300 nm), is clearly visible which again confirms the presence of this chromophore at the $\alpha$-chain end. Furthermore, the superposition of the absorption due to the thiocarbonylthio group at the $\omega$-chain-end (which extends to 400 nm) is also visible. The fluorescence spectra of both PBTP and Phe-PDcA macroCTA also show the characteristic features of phenanthrene. However, the dithiobenzoate group is an efficient quencher of the phenanthrene fluorescence [65]. The decay of the amino-derivative of phenanthrene in methanol is a single exponential ($\tau = 47$ ns) while in Phe-PDcA polymer, phenanthrene has a multi-exponential decay with a smaller average lifetime of $<\tau> = 15$ ns. In the PBTP RAFT agent, the proximity of the dithiobenzoate group adds a dynamic quenching ($<\tau> = 4$ ns) and a static quenching appears responsible for the strong decrease in fluorescence intensity observed on Fig. 5. Similar effects have been previously observed for different dye-labeled RAFT agents, either by intramolecular or by intermolecular quenching [39,65]. The quenching is lower in Phe-PDcA, as seen by the much higher fluorescence intensity in Fig. 5 (for the same absorbance values), probably due to a larger distance between the fluorophore and the thiocarbonylthio moiety compared to PBTP.

From the absorbance at 299 nm of a solution of Phe-PDcA of known mass concentration ($C_{\text{mass}}$), and using the molar extinction

**Table 2**
Polymer number average molecular weight, average degree of polymerization ($X_n$) and polydispersity index of Phe-PDcA sample corresponding to 21% conversion.

| | $^1$H NMR | UV–vis[a] | MALDI-TOF MS | SEC[b] |
|---|---|---|---|---|
| $X_n$ | 9.4 | 7.5 | 10.7 | 11.3 |
| $M_n$/g mol$^{-1}$ | 2445 | 2050 | 2720 | 2950 |
| $M_w/M_n$ | – | – | 1.13 | 1.09 |

[a] Using $\varepsilon^{299}_{\text{PBTP}} = 22,400$ mol$^{-1}$L cm$^{-1}$.
[b] SEC in THF using polystyrene standards.

**Table 3**
Experimental conditions for the synthesis of Phe-PDcA-*b*-PDEA block copolymers in the presence of Phe-PDcA macroCTA ($M_n = 2720\ g\ mol^{-1}$, $M_w/M_n = 1.13$) in 1,4 dioxane at 70 °C.

| Run | [DEA]/[Phe-PDcA] | [DEA]/M | [Phe-PDcA]/[V-65] |
|---|---|---|---|
| 1 | 880 | 3.8 | 9 |
| 2 | 445 | 3.9 | 9 |
| 3 | 140 | 3.8 | 9 |

coefficient of PBTP at the same wavelength ($\varepsilon^{299}_{PBTP} = 22,400\ mol^{-1}\ L\ cm^{-1}$), a $M_n$ of $2050\ g\ mol^{-1}$ was estimated, corresponding to $X_n = 7.5$. The lower value of $M_n$ is essentially due to the differences in the $\varepsilon$ values of PBTP and Phe-PDcA at 299 nm. Indeed, although the dithiobenzoate group is identical in both compounds, it is closer to the phenanthrene moiety in PBTB than in Phe-PDcA, which enhances the formation of ground-state phenanthrene–dithiobenzoate complexes in the former [65]. These complexes should have a small absorbance at 299 nm, which implies that the compound forming more ground-state complexes has a lower effective molar extinction coefficient. In our case, the molar extinction coefficient of PBTP at 299 nm is smaller than the corresponding value of Phe-PDcA ($\varepsilon^{299}_{macroCTP} = 29,740\ mol^{-1}\ L\ cm^{-1}$), which explains the lower values of $X_n$ determined by UV–Vis.

Table 2 summarizes the number average molecular weights, $M_n$, determined by $^1$H NMR, UV/Vis, MALDI-TOF MS and SEC. The polydispersity, $M_w/M_n$, obtained by SEC in THF using polystyrene standards and by MALDI-TOF mass spectrometry are identical.

### 3.3. Synthesis of poly(N-decylacrylamide-b-N,N-diethylacrylamide) amphiphilic block copolymers labeled with phenanthrene at the α-end (Phe-PDcA-b-PDEA)

Phe-PDcA-*b*-PDEA amphiphilic block copolymers were synthesized by sequential RAFT polymerization, using Phe-PDcA polymer ($M_n = 2720\ g\ mol^{-1}$) as macroCTA. Three runs were performed in order to obtain (five) block copolymers with exactly the same hydrophobic PDcA block length and increasing hydrophilic PDEA block lengths, according to Scheme 2. V-65 azo-initiator was chosen instead of AIBN since high MW poly(*N*-acryloylmorpholine) chains could be synthesized with this fast decomposing initiator, at a reasonable polymerization rate and with a good MW control at moderate temperature (60–70 °C) [73]. The experimental conditions are summarized in Table 3.

A conversion higher than 50% was reached in approximately 1 h (Fig. 6). In order to determine the molecular weight distributions of the Phe-PDcA-*b*-PDEA block copolymers, SEC was carried out in DMF using a multi-angle light scattering detector. Fig. 7 shows the normalized SEC traces for the first block and BC3 block copolymer, as well as the MW evolution for the five block copolymers. The clear shift towards higher MW confirmed the formation of the second block with a very low amount of dead chains from the first block, indicating a very high ω-end functionalization of the first block by the dithiobenzoate moiety and a very high blocking efficiency. From the SEC traces, the absolute molecular weights and the polydispersity indices ($M_w/M_n$) were determined considering the specific refractive index increment for the PDcA-*b*-PDEA block copolymers equal to the corresponding value for PDEA homopolymer ($dn/dC = 0.081\ mL\ g^{-1}$), which can be considered as a rather good approximation. All copolymers (BC1–BC5) have the same hydrophobic block length and different hydrophilic block lengths ranging from *ca.* 100 to 600 DEA units (Table 4).

In order to estimate the amount of polymer chains that do not bear a phenanthrene moiety at the α-chain-end (chains initiated by the initiator), the number average molecular weight, $M_n$, was calculated from the UV/Vis absorption spectrum using the molar extinction coefficient determined for Phe-PDcA homopolymer ($\varepsilon = 29{,}740\ mol^{-1}\ L\ cm^{-1}$ at 299 nm, sample of $M_n = 2720\ g\ mol^{-1}$ from MALDI-TOF MS). The effect of ground-state complex formation previously described is expected to be less important here, because of the larger distance between the fluorophore and the quencher in both the macroCTA and the block copolymers. Considering that all the copolymer chains bear a phenanthrene and a dithiobenzoate group respectively at the α- and ω-ends, the $M_n$ values were determined by UV/Vis (Table 4). For all samples, the values are larger than those obtained by SEC/MALS which are very close to the theoretical values estimated from Eq. (2). This could mean that a certain amount of chains were not α-end labeled with phenanthrene, which is expected since some polymer chains (~10%) are initiated by the V-65 initiator. However, we cannot discard the influence of differences in the molar extinction coefficients at 299 nm between the macroCTA and the block copolymers, owing to dissimilar ground-state association constants for both structures.

Fig. 8 shows the $^1$H NMR spectrum of the phenanthrene end-labeled Phe-PDcA-*b*-PDEA block copolymer BC1 (Table 4) with the corresponding proton assignment. The $^1$H NMR spectra of block copolymers are frequently used to determine their number average

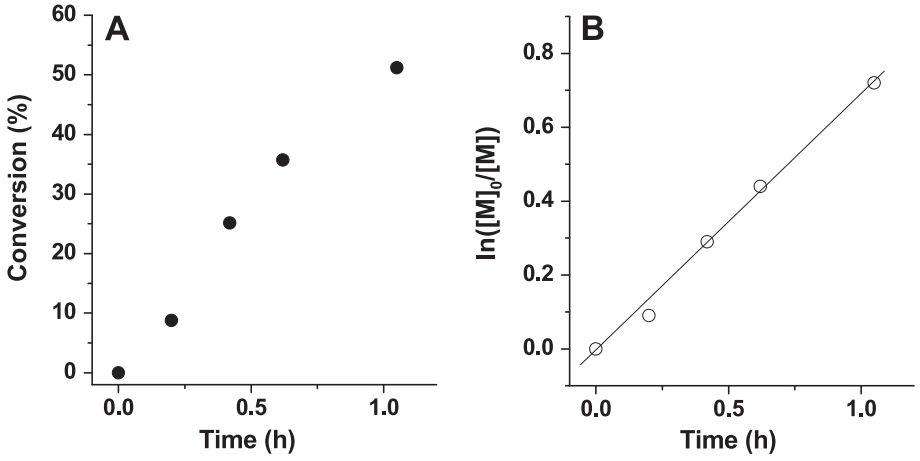


**Fig. 6.** Monomer conversion *vs* time (A) and pseudo-first order kinetics (B) for DEA polymerization in 1,4-dioxane at 70 °C using Phe-PDcA as macroCTA (run 2 in Table 3).

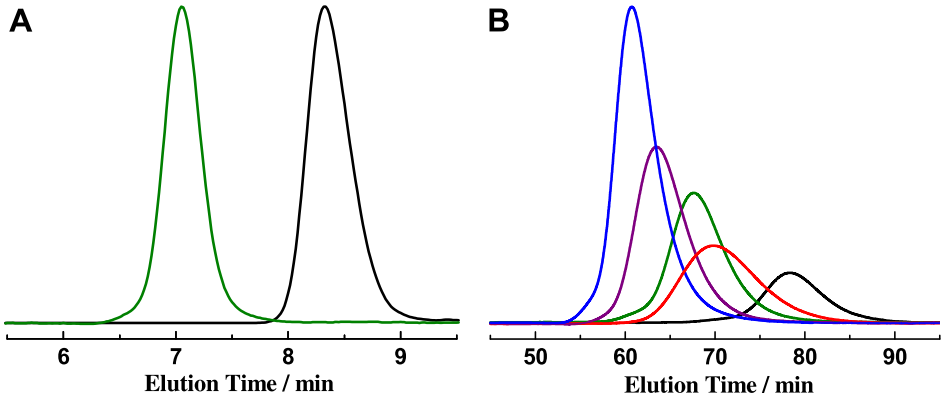


**Fig. 7.** (A) Normalized SEC traces in THF of BC3 block copolymer (left) and Phe-PDcA first block (right). (B) SEC traces in DMF using SEC-MALS for block copolymers (from BC1 on the right to BC5 on the left).

molecular weight, knowing the polymerization degree of the first block. Here, we show that this method presents some limitations. Dividing the $^1$H NMR spectrum of Phe-PDcA-*b*-PDEA (BC1) in two independent parts, A and B, and considering the average polymerization degree of the first block, $X_n = 11$, the average degree of polymerization of the hydrophilic block, $X_m$, is given by Eq. (3)

$$X_m = \frac{242 - 25I_B/I_A}{4I_B/I_A - 9} \quad (3)$$

where IB/IA is the ratio of the integrals corresponding to the A and B parts

However, the values of $X_m$ calculated with Eq. (3) have large associated errors. In fact, when the value of $I_B/I_A$ is lower than *ca.* 9/4, the error associated with the degree of polymerization, $\sigma(X_m)$, is much larger than the uncertainty in the integrals $\sigma(I_B/I_A)$

$$\frac{\sigma(X_m)}{\sigma(I_B/I_A)} = \frac{743}{(9 - 4I_B/I_A)^2} \quad (4)$$

The simulated values of $X_m$ calculated by Eq. (3) and plotted in Fig. 9A show that for $I_B/I_A < 2.5$ a small change in $I_B$ will produce a large effect in the value of $X_m$. In fact, the ratio $\sigma(X_m)/\sigma(I_B/I_A)$ from Eq. (4) increases steeply for small values of $I_B/I_A$ (Fig. 9B).

Generally, the uncertainty in the determination of the molecular weight of the second block by NMR depends on the overlap of the proton resonances of the two blocks and the relative lengths of the blocks. This uncertainty will be high for larger overlaps and when the first block is much shorter than the second block. In the present case, we could only get reliable NMR results for the shorter BC1 copolymer ($M_n = 11{,}760$ g mol$^{-1}$, $X_m = 80$).

### *3.4. Self-assembly of the Phe-PDcA-b-PDEA block copolymers in water*

The self-assembly of amphiphilic block copolymers in water, above the critical micelle concentration (CMC), is driven by the hydrophobic effect [74]. The micellar aggregates formed in aqueous solutions consist in a core of water-insoluble segments, surrounded by a stabilizing corona (or shell) formed of hydrated hydrophilic segments. The amphiphilic PDcA-*b*-PDEA block copolymers (BC1–BC5) have a relatively short PDcA hydrophobic block ($X_n = 11$), which is maintained constant, while the long PDEA hydrophilic block varies for each copolymer ($X_m = 79$–$468$), as shown in Table 4. These copolymers undergo self-assembly in water above their CMC value into regular micelle-like assemblies [75]. Fig. 10 shows the fluorescence spectra of solutions of increasing polymer concentration ($1.2 \times 10^{-7}$ M to $1.5 \times 10^{-5}$ M) with a constant concentration of anthracene ($10^{-5}$ M) at an excitation wavelength of 295 nm.

Each spectrum is a superposition of the spectrum of phenanthrene (between 345 and 420 nm) with the spectrum of anthracene (between 380 nm and 450 nm). By excitation at 295 nm, the light is absorbed by both phenanthrene and anthracene according to the corresponding optical densities at the excitation wavelength. By increasing the concentration of polymer, the concentration of phenanthrene also increases (each chain bears one phenanthrene at the PDcA chain-end) and the fraction of light absorbed by phenanthrene increases because the concentration of anthracene is maintained constant ($10^{-5}$ M). Then, in the absence of FRET, the anthracene fluorescence is expected to decrease with the increase in polymer concentration. However, as shown on Fig. 10, the anthracene fluorescence intensity increases which points to the possibility of energy transfer from phenanthrene to anthracene. This does not occur before the formation of micelles because the anthracene

**Table 4**
Number average molecular weight ($M_n$) and polydispersity indices ($M_w/M_n$) for the Phe-PDcA-*b*-PDEA block copolymers, and average degree of polymerization ($X_m$) of the PDEA block, for DEA polymerization using a Phe-PDcA macroCTA ($M_n = 2720$ g mol$^{-1}$, $M_w/M_n = 1.13$) in 1,4 dioxane at 70 °C.

| Entry | Run | Conv./% | Expected | | UV/Vis[a] | | SEC-MALS | | Exp. % Dye |
|---|---|---|---|---|---|---|---|---|---|
| | | | $X_m$ | $M_n$/g mol$^{-1}$ | $X_m$ | $M_n$/g mol$^{-1}$ | $X_m$ | $M_n$/g mol$^{-1}$ ($M_w/M_n$) | |
| BC1 | 3 | 60 | 82 | 13190 | 96 | 15,000 | 79 | 12,700 (1.01) | 85 |
| BC2 | 1 | 16 | 144 | 21035 | 183 | 26,000 | 146 | 21,200 (1.05) | 82 |
| BC3 | 2 | 51 | 228 | 31760 | 247 | 34,100 | 227 | 31,600 (1.03) | 93 |
| BC4 | 1 | 37 | 330 | 44725 | 391 | 52,500 | 295 | 40,300 (1.01) | 78 |
| BC5 | 1 | 56 | 497 | 65895 | 602 | 79,200 | 468 | 62,300 (1.02) | 79 |

[a] Using $\varepsilon$ (299 nm) = 29,740 mol$^{-1}$ L cm$^{-1}$ for the macroCTA.

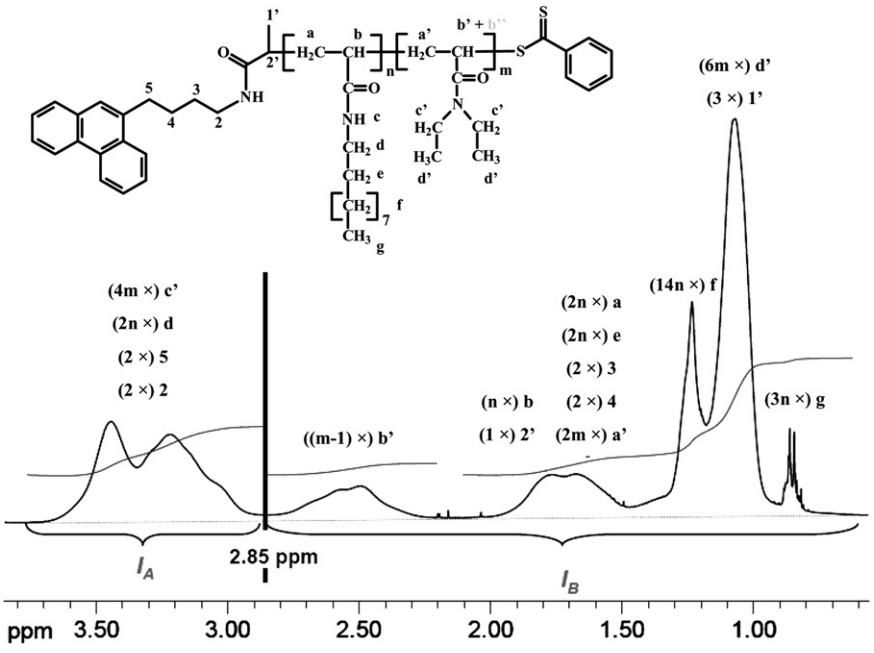


**Fig. 8.** $^1$H NMR spectrum of Phe-PDcA-*b*-PDEA block copolymer (BC1) in $CDCl_3$ and protons assignment.

concentration in the bulk solution is very low. However, after the formation of micelles, the anthracene migrates to the core of the micelles where the phenanthrene is also located, originating energy transfer from phenanthrene to anthracene and the consequent increase of the fluorescence intensity of anthracene.

Fig. 11 shows the fluorescence intensity of anthracene recorded at 425 nm, corrected by Eq. (5), for the amount of excitation light absorbed within the sample cell and the repartition of the absorption between phenanthrene and anthracene [76].

$$I_{An}(\text{Corrected}) = I_{An} \times \frac{\varepsilon_{An}^{295} c_{An} + \varepsilon_{Phe}^{295} c_{Phe}}{\varepsilon_{An}^{295} c_{An}} \times \frac{1}{1 - \exp\left[-2.303\left(\varepsilon_{An}^{295} c_{An} + \varepsilon_{Phe}^{295} c_{Phe}\right) l\right]} \quad (5)$$

where $\varepsilon_i^{295}$ is the molar extinction coefficient of compound $i$ at 295 nm and $c_i$ is the corresponding concentration and $l$ is the optical path length of the cell. The molar extinction coefficients of the phenanthrene-labeled polymer and anthracene in water are almost impossible to obtain due to the very low solubility of these compounds. Fortunately, the molar extinction coefficients of both compounds do not vary significantly from nonpolar to polar solvents. Then, we consider for anthracene the value in cyclohexane ($\varepsilon_{An}^{295} = 520\ \text{mol}^{-1}\,\text{L}\,\text{cm}^{-1}$) and for the phenanthrene-labeled polymer, the value found for the model compound, phenanthrene-9-methyl acetate, in cyclohexane ($\varepsilon_{An}^{295} = 11{,}100\ \text{mol}^{-1}\,\text{L}\,\text{cm}^{-1}$) [77].

The corrected fluorescence intensity of anthracene is almost constant for low polymer concentrations and increases afterwards, as shown in Fig. 11.

The anthracene fluorescence intensity increase is due to energy transfer from phenanthrene to anthracene that can only occur after the formation of micelles, when both fluorophores are located in the micelle core. Then, the intersection of the two lines before and after the formation of micelles gives the critical micelle concentration,

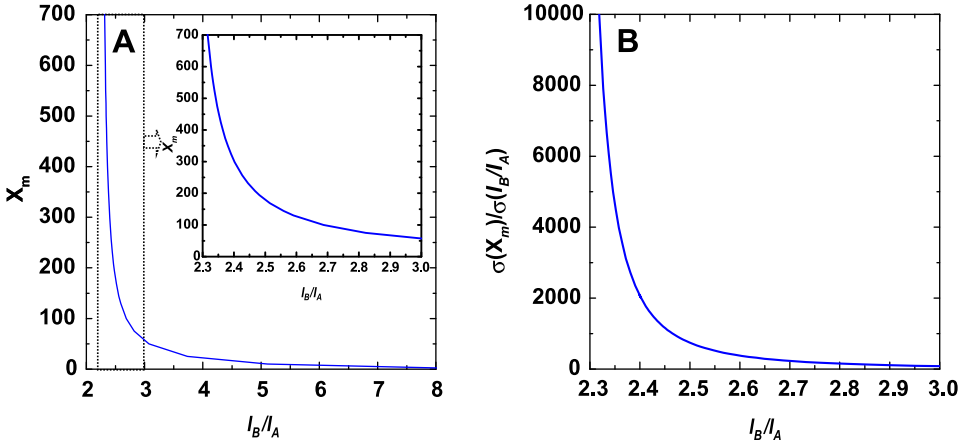


**Fig. 9.** (A) Plot of the expected values of the degree of polymerization of the PDEA block as a function of the integral ratio $I_B/I_A$ (enlarged in the *inset*). (B) Plot of the ratio of $X_m$ and $I_B/I_A$ errors as a function of $I_B/I_A$.

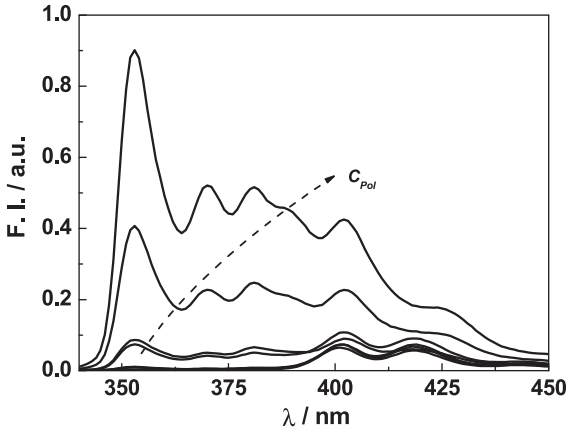


**Fig. 10.** Fluorescence spectra of phenanthrene-labeled BC4 polymer solutions for several concentrations of polymer ($1.2 \times 10^{-7}$ M–$1.5 \times 10^{-5}$ M) and a fixed concentration of anthracene ($10^{-5}$ M).

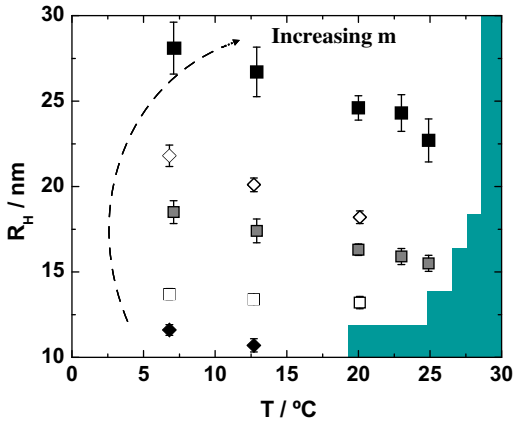


**Fig. 12.** Hydrodynamic radii of the micellar aggregates formed by PDcA-*b*-PDEA block copolymers (BC1–BC5) in water determined at several temperatures by DLS and volume phase transition temperatures, $T_{VPT}$, of each copolymer indicated by the temperature at the border line of the grey region. The concentration of each copolymer was [BC] ≈ 1.4 g $L^{-1}$.

CMC = 0.063 g $L^{-1}$ = 1.6 μM. The CMC is low compared to the usual values for micelles of common surfactants but close to the values reported for polymer micelles in several solvents [48,74,78]. Similar values were obtained for the other copolymers, irrespective of the length of the hydrophilic block.

Fig. 12 shows the hydrodynamic radii ($R_H$) of the micellar structures obtained by DLS at several temperatures. The micellar radii ($R_H$) vary with the length of the hydrophilic block, longer hydrophilic blocks leading to larger micelles. Moreover, $R_H$ values slightly decrease in response to temperature increase due to the volume phase transition (VPT) of the shell that occurs near the LCST (~32 °C) of PDEA in water. This variation with temperature is more pronounced for the larger micellar aggregates.

Above the LCST of the PDEA, the light scattering of the solution increases drastically as well as the turbidity of the sample due to the formation of large aggregates (Fig. 12, grey region) which are probably multi-micellar aggregates. These aggregates are formed since the PDEA corona shrinks and becomes less hydrophilic, which decreases the stability of the micelles in aqueous solution. The sizes of the aggregates are relatively large to be determined accurately by DLS (>1 μm). Similar observations were reported for pH responsive polymers [79]. Moreover, the aggregation is reversible since the turbidity disappears by cooling the solution to temperatures below $T_{VPT}$. DLS measurements indicate the presence of two populations, one of large aggregates (due to some flocculation) and other of micellar aggregates with hydrodynamic radii close to those before heating.

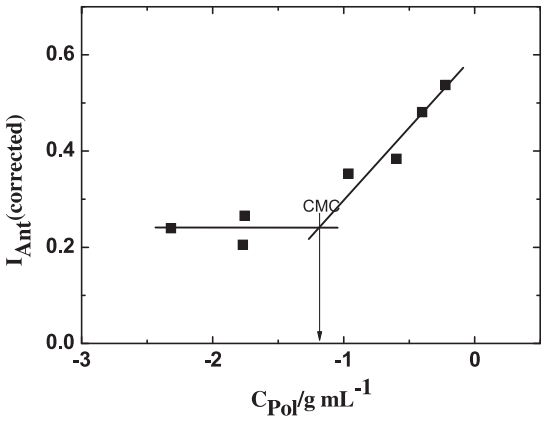


**Fig. 11.** Plot of the corrected fluorescence intensity of anthracene ($10^{-5}$ M) for phenanthrene-labeled BC4 polymer solutions of increasing concentration.

## 4. Conclusion

Phenanthrene-labeled poly(*N*-decylacrylamide-*b*-*N*,*N*-diethylacrylamide) block copolymers were synthesized using a new phenanthrene-labeled RAFT agent. A straightforward approach was used to prepare the fluorescent RAFT agent, *N*-[4-(9-phenanthrenyl)butyl-2-(2-phenyl-1-thioxo)thio]-propanamide (PBTP) in a high yield and with a very stable amido linkage connecting the phenanthrene to the thiocarbonylthio moiety. This new RAFT agent efficiently controlled the polymerization of a hydrophobic acrylamide derivative (*N*-decylacrylamide). Furthermore, the resulting polymer bearing a phenanthrene moiety at the α-chain-end and a thiocarbonylthio moiety at the ω-chain-end was used as macroCTA to polymerize *N*,*N*-diethylacrylamide. Using this sequential approach, several block copolymers with the same PDcA hydrophobic block and PDEA blocks of several lengths were prepared and characterized. These copolymers self-assemble in water forming thermoresponsive micelles, with CMC values around 2 μM. The radius of the micelles decrease with temperature increase around the LCST of PDEA in water, due to the volume phase transition of the PDEA shell, the decrease being more pronounced for the micelles with longer PDEA blocks.

## Acknowledgments

The authors thank Dr Maël Bathfield (Unité Mixte CNRS-bioMérieux) for the synthesis of the precursor RAFT agent, as well as Dr Catherine Ladavière (Unité Mixte CNRS-bioMérieux) and Frédéric Delolme (SCA, CNRS, Solaize, France) for the MALDI-ToF MS analyses and interesting discussions. Telmo Prazeres and Mariana Beija thank FCT for the SFRH/BD/5095/2001 and SFRH/BD/18562/2004 grants, respectively.

## References

[1] (a) Maliakal A, Greenaway H, O'Shaughnessy B, Turro NJ. Macromolecules 2003;36:6075;
(b) Martinho JMG, Sienicki K, Blue D, Winnik MA. J Am Chem Soc 1988;110:7773;
(c) Stukelj M, Martinho JMG, Winnik MA, Quirk RP. Macromolecules 1991;24:2488;
(d) Sisido M, Imanishi Y, Higashimura T. Macromolecules 1979;12:975.

[2] (a) Martinho JMG, Winnik MA. Macromolecules 1986;19:2281;
(b) Boileau S, Méchin F, Martinho JMG, Winnik MA. Macromolecules 1989;22:215.
[3] Winnik MA. Acc Chem Res 1985;18:73.
[4] Xu J, Zhu ZY, Luo SZ, Wu C, Liu SY. Phys Rev Lett 2006;96:027802.
[5] (a) Piçarra S, Duhamel J, Fedorov A, Martinho JMG. J Phys Chem B 2004;108:12009;
(b) Piçarra S, Relógio P, Afonso CAM, Martinho JMG, Farinha JPS. Macromolecules 2003;36:8119 (correction: Piçarra S, Relógio P, Afonso CAM, Martinho JMG, Farinha JPS. Macromolecules 2004;37: 1670);
(c) Farinha JPS, Piçarra S, Miesel K, Martinho JMG. J Phys Chem B 2001;105:10536;
(d) Piçarra S, Gomes PT, Martinho JMG. Macromolecules 2000;33:3947.
[6] Irondi K, Zhang MZ, Duhamel J. J Phys Chem B 2006;110:2628.
[7] (a) Farinha JPS, Schillen K, Winnik MA. J Phys Chem B 1999;103:2487;
(b) Schillen K, Yekta A, Ni SR, Farinha JPS, Winnik MA. J Phys Chem B 1999;103:9090.
[8] (a) Yang J, Lou XD, Spiro JG, Winnik MA. Macromolecules 2006;39:2405;
(b) Ye XD, Farinha JPS, Oh JK, Winnik MA, Wu C. Macromolecules 2003;36:8749;
(c) Farinha JPS, Spiro JG, Winnik MA. J Phys Chem B 2001;105:4879;
(d) Farinha JPS, Vorobyova O, Winnik MA. Macromolecules 2000;33:5863;
(e) Pham HH, Farinha JPS, Winnik MA. Macromolecules 2000;33:5850.
[9] Beija M, Relógio P, Charreyre MT, da Silva AMG, Brogueira P, Farinha JPS, et al. Langmuir 2005;21:3940.
[10] (a) Callahan J, Kopecek J. Biomacromolecules 2006;7:2347;
(b) Jiang JQ, Tong X, Zhao Y. J Am Chem Soc 2005;127:8290;
(c) Rapoport N, Marin A, Luo Y, Prestwich GD, Muniruzzaman M. J Pharm Sci 2002;91:157.
[11] Trenor SR, Shultz AR, Love BJ, Long TE. Chem Rev 2004;104:3059.
[12] Winnik FM. Chem Rev 1993;93:587.
[13] Vangani V, Duhamel J, Nemeth S, Jao TC. Macromolecules 1999;32:2845.
[14] Wang MF, Dykstra TE, Lou XD, Salvador MR, Scholes GD, Winnik MA. Angew Chem Int Ed 2006;45:2221.
[15] Tong JD, Ni SR, Winnik MA. Macromolecules 2000;33:1482.
[16] Martin TJ, Webber SE. Macromolecules 1995;28:8845.
[17] (a) Zettl H, Hafner W, Boker A, Schmalz H, Lanzendorfer M, Muller AHE, et al. Macromolecules 2004;37:1917;
(b) Sukhishvili SA, Chen Y, Muller JD, Gratton E, Schweizer KS, Granick S. Macromolecules 2002;35:1776.
[18] Horinaka J, Maruta M, Ito S, Yamamoto M. Macromolecules 1999;32:1134.
[19] (a) Horinaka J, Amano S, Funada H, Ito S, Yamamoto M. Macromolecules 1998;31:1197;
(b) Ono K, Ueda K, Yamamoto M. Polymer J 1994;26:1345;
(c) Yokotsuka S, Okada Y, Tojo Y, Sasaki T, Yamamoto M. Polymer J 1991; 23:95;
(d) Hyde PD, Waldow DA, Ediger MD, Kitano T, Ito K. Macromolecules 1986;19:2533;
(e) Valeur B, Monnerie L. J Polym Sci Polym Phys Ed 1976;14:11;
(f) Sasaki T, Yamamoto M, Nishijima Y. Makromol Chem Rapid Commun 1986;7:345.
[20] (a) Braunecker WA, Matyjaszewski K. Prog Polym Sci 2007;32:93;
(b) Hawker CJ, Bosman AW, Harth E. Chem Rev 2001;101:3661;
(c) Matyjaszewski K, Xia J. Chem Rev 2001;101:2921;
(d) Kamigaito M, Ando T, Sawamoto M. Chem Rev 2001;101:3689;
(e) Moad G, Rizzardo E, Thang SH. Aust J Chem 2005;58:349;
(f) Perrier S, Takolpuckdee P. J Polym Sci Part A Polym Chem 2005;43:5347;
(g) Favier A, Charreyre MT. Macromol Rapid Commun 2006;27:653.
[21] Odian GG. Principles of polymerization. 4th ed. Hoboken, NJ: Wiley-Interscience; 2004.
[22] Nakayama M, Okano T. Biomacromolecules 2005;6:2320.
[23] Scales CW, Convertine AJ, McCormick CL. Biomacromolecules 2006;7:1389.
[24] York AW, Scales CW, Huang F, McCormick CL. Biomacromolecules 2007; 8:2337.
[25] Segui F, Qiu XP, Winnik FM. J Polym Sci Part A Polym Chem 2008;46:314.
[26] Harth E, Hawker CJ, Fan W, Waymouth RM. Macromolecules 2001;34:3856.
[27] O'Bryan G, Braslau R. Macromolecules 2006;39:9010.
[28] Zhou P, Chen GQ, Hong H, Du FS, Li ZC, Li FM. Macromolecules 2000;33:1948.
[29] Wang XF, Zhang YF, Zhu ZY, Liu SY. Macromol Rapid Commun 2008;29:340.
[30] Chen F, Cheng ZP, Zhu J, Zhang W, Zhu XL. Eur Polym J 2008;44:1789.
[31] Rodlert M, Harth E, Rees I, Hawker CJ. J Polym Sci Part A Polym Chem 2000;38:4749.
[32] Gavranovic GT, Csihony S, Bowden NB, Hawker CJ, Waymouth RM, Moerner WE, et al. Macromolecules 2006;39:8121.
[33] Lindner SM, Thelakkat M. Macromol Chem Phys 2006;207:2084.
[34] Bucsiova L, Yin MZ, Chmela S, Habicher WD. J Macromol Sci Part A Pure Appl Chem 2008;45:761.
[35] Duan Q, Miura Y, Narumi A, Sato SI, Satoh T, Kaga H, et al. J Polym Sci Part A Polym Chem 2006;44:1117.
[36] Lu X, Zhang L, Meng L, Liu Y. Polym Bull 2007;59:195.
[37] Ohno K, Fujimoto K, Tsujii Y, Fukuda T. Polymer 1999;40:759.
[38] Bowden NB, Willets KA, Moerner WE, Waymouth RM. Macromolecules 2002;35:8122.
[39] Chen M, Ghiggino KP, Mau AWH, Rizzardo E, Thang SH, Wilson GJ. Chem Commun 2002:2276.
[40] Chen M, Ghiggino KP, Mau AWH, Rizzardo E, Sasse WHF, Thang SH, et al. Macromolecules 2004;37:5479.
[41] Chen M, Ghiggino KP, Mau AWH, Sasse WHF, Thang SH, Wilson GJ. Macromolecules 2005;38:3475.
[42] Fu J, Cheng ZP, Zhou N, Zhu J, Zhang W, Zhu X. Polymer 2008;49:5431.
[43] Mertoglu M, Laschewsky A, Skrabania K, Wieland C. Macromolecules 2005;38:3601.
[44] (a) Bathfield M, D'Agosto F, Spitz R, Charreyre MT, Delair T. J Am Chem Soc 2006;128:2546;
(b) Bathfield M, Daviot D, D'Agosto F, Spitz R, Ladavière C, Charreyre MT, et al. Macromolecules 2008;41:8346.
[45] Lowe AB, McCormick CL. Prog Polym Sci 2007;32:283.
[46] McCormick CL, Lowe AB. Acc Chem Res 2004;37:312.
[47] Relógio P, Charreyre MT, Farinha JPS, Martinho JMG, Pichot C. Polymer 2004;45:8639.
[48] de Lambert B, Charreyre MT, Chaix C, Pichot C. Polymer 2007;48:437.
[49] (a) Favier A, Charreyre MT, Pichot C. Polymer 2004;45:8661;
(b) Favier A, D'Agosto F, Charreyre MT, Pichot C. Polymer 2004;45:7821.
[50] Favier A, Charreyre MT, Chaumont P, Pichot C. Macromolecules 2002;35:8271.
[51] Zana R. J Phys Chem B 1999;103:9117.
[52] Maeda Y, Nakamura T, Ikeda I. Macromolecules 2002;35:10172.
[53] Eggert M, Freitag R. J Polym Sci Part A Polym Chem 1994;32:803.
[54] Kobayashi M, Ishizone T, Nakahama S. J Polym Sci Part A Polym Chem 2000;38:4677.
[55] Garret-Flaudy F, Freitag R. Langmuir 2001;17:4711.
[56] Liu HY, Zhu XX. Polymer 1999;40:6985.
[57] Bromberg L, Levin G. Bioconjug Chem 1998;9:40.
[58] Bromberg L, Levin G. Macromol Rapid Commun 1998;19:79.
[59] Panayiotou M, Freitag R. Polymer 2005;46:6777.
[60] Panayiotou M, Freitag R. Polymer 2005;46:615.
[61] D'Agosto F, Charreyre MT, Pichot C. Macromol Biosci 2001;1:322.
[62] Afonso CAM, Farinha JPS. J Chem Res Synop 2002;584.
[63] D'Agosto F, Charreyre MT, Veron L, Llauro MF, Pichot C. Macromol Chem Phys 2001;202:1689.
[64] Favier A, Ladaviere C, Charreyre MT, Pichot C. Macromolecules 2004;37:2026.
[65] Farinha JPS, Relógio P, Charreyre MT, Prazeres TJV, Martinho JMG. Macromolecules 2007;40:4680.
[66] (a) Castro E, Barbosa S, Juárez J, Taboada P, Katime IA, Mosquera V. J Phys Chem B 2008;112:5296;
(b) Castro E, Taboada P, Mosquera V. J Phys Chem B 2006;110:13113.
[67] (a) Zhou N, Lu L, Zhu J, Yang X, Wang X, Zhu X, et al. Polymer 2007;48:1255;
(b) Chen M, Ghiggino KP, Launikonis A, Mau AWH, Rizzardo E, Sasse WHF, et al. J Mater Chem 2003;13:2696;
(c) Chen M, Ghiggino KP, Thang SH, Wilson GJ. Angew Chem Int Ed 2005;44:4368;
(d) Chen M, Ghiggino KP, Thang SH, White J, Wilson GJ. J Org Chem 2005;70:1844;
(e) Such GK, Evans RA, Davis TP. Macromolecules 2006;39:9562.
[68] (a) Zhu J, Zhu XL, Zhou D, Chen JY, Wang XY. Eur Polym J 2004;40:743;
(b) Zhu J, Zhu XL, Cheng ZP, Liu F, Lu JM. Polymer 2002;43:7037;
(c) Li Y, Yang JW, Benicewicz BC. J Polym Sci Part A Polym Chem 2007;45:4300;
(d) Wan XM, Zhu XL, Zhu J, Zhang ZB, Cheng ZP. J Polym Sci Part A Polym Chem 2007;45:2886.
[69] The CTA and the targeted $M_n$ are different, however we have previously shown [49] that the kinetics of the RAFT polymerization of acrylamide derivatives mediated by dithiobenzoates at 90 °C is identical for various targeted $M_n$ once the CTA/AIBN ratio is kept constant.
[70] de Lambert B, Charreyre MT, Chaix C, Pichot C. Polymer 2005;46:623.
[71] (a) Schilli C, Lanzendorfer MG, Muller AHE. Macromolecules 2002;35:6819;
(b) Toy AA, Vana P, Davis TP, Barner-Kowollik C. Macromolecules 2004;37:744;
(c) Destarac M, Charmot D, Franck X, Zard SZ. Macromol Rapid Commun 2000;21:1035.
[72] Vana P, Albertin L, Barner L, Davis TP, Barner-Kowollik C. J Polym Sci Part A Polym Chem 2002;40:4032.
[73] Charreyre MT, Favier A. WO 04/055060; 2004.
[74] Riess G. Prog Polym Sci 2003;28:1107.
[75] Marcelo G, Prazeres TJV, Charreyre MT, Martinho JMG, Farinha JPS. Macromolecules in press, doi:10.1021/ma902103q.
[76] Conte JC, Martinho JMG. J Lumin 1981;22:273.
[77] Liu R, Moffitt M, Winnik MA, Heinemann J, Mülhaupt R. J Polym Sci Part A Polym Chem 1990;37:4169.
[78] Evans DF, Wennerström H. The colloidal domain. Where physics chemistry, biology, and technology meet. 2nd ed. NY: Wiley-VCH; 1999.
[79] Gao LC, Shi LQ, Zhang WQ, An YL, Jiang XW. Macromol Chem Phys 2006; 207:521.